COMPARISON OF TWO TYPES OF ANDREEV REFLECTION HOT-ELECTRON MICROBOLOMETER FOR SUBMILLIMETER RADIO ASTRONOMY

A.N. Vystavkin

Institute of Radioengineering and Electronics of RAS, 11 Mokhovaya Str., Moscow 103907, Russia

Review and analysis of results of theoretical estimations and measurements of characteristics of an Andreev reflection hot-electron direct detection microbolometer for submillimeter radio astronomy made by different researchers are given. The consideration is limited to the case when minimized in dimensions absorber of the microbolometer is antenna-coupled and together with antenna are deposited directly onto substrate without a membrane or spider-web and cooled to approximately 100 mK what provides the best noise equivalent power. A comparison of peculiarities and characteristics of the microbolometers using two types of sensors - the SIN-junction sensor and the transition-edge sensor (TES) with electrothermal feedback - for the read-out of a signal arising from the electron temperature increment under the influence of submillimeter radiation is presented. Advantages of the microbolometer with the second type of the sensor when the TES is used simultaneously as the absorber of radiation are shown. Methods of achievement of the best noise equivalent power of the microbolometer in such version as well as methods of the matching of the microbolometer with the incident radiation flow and with the channel of the output signal read-out are considered.

1. Introduction.

One of the fundamental problems of the contemporary radio astronomy [1-3] is the problem of the investigation of a celestial sphere electromagnetic radiation in the frequency region 0.3 - 3.0 THz as a result of what they are expecting an abundant information which will bring us forward to the significant broadening of our ideas about the Universe. To attack this problem besides highsensitive narrowband superheterodyne receivers [4] the broadband receivers of direct detection type, most sensitive among which are the receivers based on hot-electron microbolometers [5-8], are necessary. The choice of two types of receivers for frequency region 0.3 - 1.5 THz [3], superheterodyne and direct detection types, is led mainly to the reason that when they are observing weak but broadband radiation sources it may occur that the sensitivity of narrowband superheterodyne receivers could be not enough and at the same time the microbolometers as direct detectors due to their very wide frequency band will detect this radiation. Besides as direct detection microbolometers do not need heterodyne pumping it is much easier to construct multi-element receiving structures on their basis for an observation spatially inhomogeneous distributed radiation sources though having not too high frequency resolution. For many tasks of the submillimeter radio astronomy the noise equivalent power (*NEP*) of direct detection microbolometers of order of 10^{-17} - 10^{-18} W$\cdot$Hz$^{-1/2}$ is necessary [1-3, 9] and for some tasks in future the *NEP* down to 10^{-20}-10^{-21} W$\cdot$Hz$^{-1/2}$ will be required [10].

2. Andreev reflection hot-electron microbolometer with a SIN-junction as the output signal read-out sensor.

Amongst mentioned above hot-electron microbolometers Andreev reflection [11] one operating at sub-Kelvin temperatures is recognized as the most promising [7, 8] because of its comparatively high sensitivity and lowest time constant. The first concept of this microbolometer was proposed in [7]. In the first experiments on the realization of this concept

[8] the microbolometer design was comparatively simple structure (the inset of Fig. 1) comprising a normal metal film (Cu) with dimensions: 6-μm- long, 0.3-μm-wide, and 75-nm-thick and lead electrodes of Al (the superconductor at temperatures <1.2 K) deposited on the silicon substrate using the electron-beam lithography and triple-angle evaporation process. A submillimeter radiation has to be absorbed by electrons in the normal metal film and heat them. However due to difficulties of the leading a radiation into the cryostat at sub-Kelvin
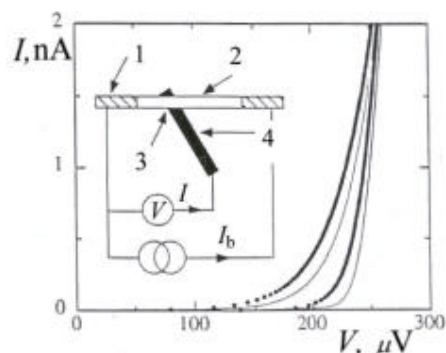

Fig. 1. *I-V* characteristics of the SIN-junction. Solid thin curves correspond to temperatures 40 mK (right) and 300 mK (left) at zero bias current through the absorber. Dotted thick curves correspond to a base temperature of 40 mK with 20 fW (right) and 2 pW (left) power dissipated in the normal metal absorber. The scheme of measurements is given at the inset. The power dissipated in the resistor R of the absorber is $I_b^2 \cdot R$: 1 - superconducting lead electrodes bringing bias current into the absorber, 2 - copper absorber, 3 - SIN-junction, 4 - superconducting electrode of SIN-junction [8].

Fig. 2. Dependence $V=f(I_b)$ at three fixed values of SIN-junction current I and temperature $T = 30$ mK for two absorber samples of 6-μm-length (curves 1) and 12-μm-length (curves 2) [12-14].

temperatures the measurements with the radiation were not made in first experiments and the heating of electrons was realized by means of the d.c. biasing. Two circumstances lead to the effective heating of electrons: (a) the superlow temperature ($\leq$0.1-0.3 K) owing to what the interaction between electrons and metal film through electron-phonon collisions and therefore the energy transfer from electrons to the absorber lattice is extremely low, and (b) the phenomenon of Andreev reflection of electrons at the normal metal - superconductor boundaries which takes place without the energy transfer of electrons to the superconducting electrodes [11]. At temperatures < 1 K the electrical resistance of the normal metal film does not depend on temperature. By this reason unlike to classic bolometers when an increment of voltage drop caused by the absorber resistance increase owing to the temperature increase due to the absorber heating is measured - in case of the described microbolometer the voltage increment at the SIN (superconductor-insulator-normal metal) junction (see Fig. 1) caused by the increment of temperature of electrons in the normal metal film is measured. This junction was made by the following way: before the deposition of the normal metal film (Cu) onto the silicon substrate the 50-nm-thick and 0.2-μm-wide strip of superconductor (Al) simultaneously with lead electrodes (also Al) were deposited under the central part of the normal metal film (to be deposited) and after that first one was oxidized [8]. *I-V* curves of the SIN-junction (examples of what are shown at Fig. 1) at different absorber film temperatures $T = T_{ph}$ and the bias currents I_b through the absorber where measured [8]. The experimental dependence of the electron
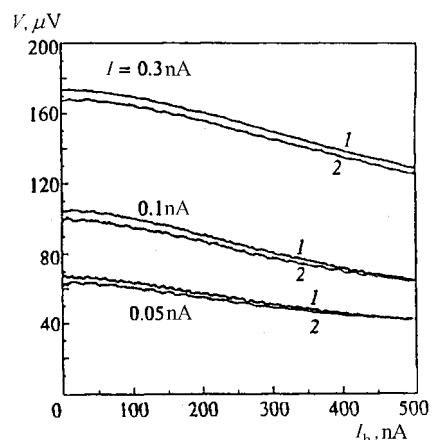
temperature T_e on the d.c. power $P = I_b^2 \cdot R$ dissipated in the absorber film was calculated from the *I-V* curves and plotted. The obtained dependence is fitted well with the theoretical dependence:

$$P_{e \to ph} = \Sigma v \,(T_e^5 - T_{ph}^5), \qquad\qquad (1)$$

where $\Sigma = 3.7$ nW $\cdot$ K$^{-5}\cdot$ mm^{-3} is fitting characteristic material parameter, and v is copper absorber film volume. It follows from good coincidence of the form of the theoretical dependence (1) and the experimental curve that a predominating mechanism of electron energy flow out is the electron energy transfer to the copper film lattice through electron-phonon interaction and other possible mechanisms of electron energy flow out do not give noticeable contribution to this process. In the same time this means that the Andreev reflection of electrons at the normal metal-superconductor boundaries takes place. A voltage responsivity calculated from the *I-V* curves is $S_V \cong 10^9$ V/W at temperature 100 mK, what is in good agreement with preliminary estimations of authors of [8]. The noise voltage measured at the input of the amplifier of SIN-junction output signal is $\sqrt{\overline{u_n^2}} \cong 3$ nV $\cdot$ Hz$^{-1/2}$ what at said above voltage responsivity corresponds to the electrical (i.e. calculated from measurements at d.c.) *NEP* of the microbolometer $NEP = \sqrt{\overline{u_n^2}} : S_V \cong 3 \cdot 10^{-18}$ W $\cdot$ Hz$^{-1/2}$.

The results similar to described above ones are obtained in [12-14]. The difference is that an absorber was fabricated not of copper but of 3-nm-thick chrome sublayer for a better adhesion with the substrate and 35-nm-thick silver layer with other dimensions of 6 - μm-length and 0.25-μm-width. Besides in said works measurements of the dependence of voltage over SIN-junction on the current I_b through the absorber at two its lengths: 6 and 12 μm and three fixed SIN-junction currents I were made (Fig. 2). Practically the dependences at two different lengths coincide. This means that the increase of the power $I_b^2 \cdot R$ dissipated in the longer absorber due to its higher resistance R has been exactly compensated by the increase of the heat conductance due to the larger volume v. This is one more confirmation that there is no substantial electron energy transport through normal metal-superconductor contacts, i.e. this is one more confirmation of the Andreev reflection at these contacts.

Initially the Andreev reflection hot-electron microbolometers with the SIN-junction sensors were used as X-ray detectors [15, 16].

3. Andreev reflection hot-electron microbolometer based on superconducting transition-edge sensor (TES) for the output signal read-out.

The application of a sensor based on superconducting transition (transition-edge sensor - TES) with strong electrothermal feedback as output signal read-out sensor for the microbolometer of described type using for detection of X-rays, neutrino and other atomic particles was proposed in [17]. In such sensor a superconductor or a bilayer of superconductor and normal metal with proximity effect is in good thermal contact with an absorber of X-rays [18], neutrino or other atomic particles. A typical electrical circuit into which the TES as the microbolometer output signal read-out sensor is connected is shown at Fig. 3 [19]. A practical circuit of the microbolometer with TES for the detection of X-rays radiation is shown at Fig. 4. Lead electrodes bringing current into the TES are made of a superconductor with significantly higher critical temperature i.e. larger energy gap in comparison with the same value of the TES

structure to provide the functioning of Andreev reflection at the boundaries of the TES and current lead electrodes. The microbolometer realized in accordance with the Fig. 4 was tested and has shown à significantly higher sensitivity to X-ray radiation [20] in comparison with the microbolometer based on SIN-junction as output signal read-out sensor of the same authors [15, 16].
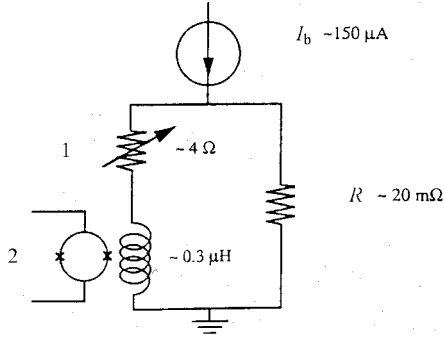

Fig. 3. Schematic of the electrical circuit used to bias the TES: 1 - TES, 2 – SQUID read-out circuit with input coil ~0.3 μH [19]. Fixed bias voltage is applied from shunt resistance $R \cong 20$ mΩ to the series connection of the TES and SQUID input coil.
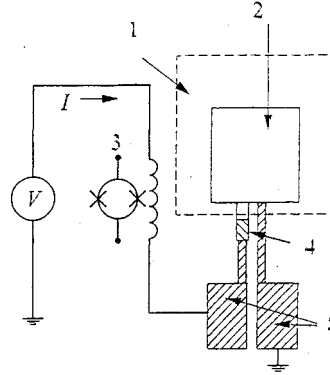
Fig. 4. Schematic of the hot-electron microbolometer for X-rays radiation measurements based on the TES with electrothermal feedback and the SQUID: 1 - Si_3N_4 membrane, 2 - silver absorber, 3 - SQUID, 4 - TES, 5 - aluminum contacts [18]. The Si_3N_4 membrane is used for the efficiency enhancement of the X-ray photon energy conversion into the electron thermal energy [15].

It is proposed in the work [20] to use the TES combined with the absorber for the detection of the submillimeter and infrared radiation. An electrical circuit into which the absorber-TES connected is the same as at Fig. 3 where 1 is now the combined absorber-TES which as in case of the normal metal absorber of the microbolometer described in the previous paragraph is deposited together with the bringing current lead electrodes onto a substrate, for instance, of silicon. Issues of the leading-in submillimeter radiation into the absorber-TES are considered below. In such version of the microbolometer the substrate with absorber-TES is cooled down to a temperature lower than the temperature of the superconducting transition. The absorber-TES is connected in series with the input coil of SQUID-picoammeter and the d.c. bias voltage V from the shunt resistance $\cong 20$ mΩ is applied across this series connection (Fig. 3). At the mode of fixed bias voltage the equilibrium amount of electron energy and consequently of electron temperature in the absorber-TES is automatically maintained at all area of the superconducting transition due to an electrothermal feedback functioning in the following way [17, 18]. During the process of absorption of the submillimeter radiation by the absorber-TES the electrons in it are heated. The TES resistance R starts to increase with the heating of the electrons and this leads to the decreasing of the dissipated Joule heat V^2/R and of course to the decreasing of the current V/R flowing through the TES. In the same moment the electron temperature returns practically to the initial value and the resistance R becomes somewhat higher. The return of electron temperature to the equilibrium value is taking place in accordance with the relation [17]:

$$C\frac{d\Delta T_e}{dt} = -\frac{P_0\alpha}{T_e}\Delta T_e - G\Delta T_e. \tag{2}$$

In the considered case when the heat coupling of electrons with the absorber-TES lattice is significantly weaker than the heat coupling of the absorber-TES lattice with the substrate lattice [17] C is electronic heat capacity, ΔT_e - electron temperature increment, $P_0 = \Sigma v T_e^5 = G T_e/5$ - equilibrium value of electron power dissipated in the absorber-TES, $G = dP/dT_e = 5\Sigma v T_e^4$ - heat conductivity from electrons to the absorber-TES lattice, $\alpha = \mathrm{d}\log R/\mathrm{d}\log T$ - the dimensionless measure of the sharpness of the superconducting transition.

In conclusion one may say that the increasing of power dissipated in the absorber-TES on account of the additional power due to the absorption of the submillimeter radiation is compensated by the decreasing of d.c. power corresponding to the Joule heat. At this time the SQUID-picoammeter measures the decreasing of current $-\Delta I$ what is the output signal of the microbolometer. In the described process the replacement of the d.c. energy by the energy of absorbed radiation takes place in the electron system and consequently this does not lead to the change of energy flow from the electrons to the absorber-TES lattice under the radiation influence. By this reason the effective time constant τ_{eff} of this process is lower of the intrinsic time constant $\tau_{e\rightarrow ph}$ caused by the energy transfer from electrons to phonons in $1+\alpha/5$ times [17].

The bilayer of aluminum and silver was used as the absorber-TES in the work [18]: 30-nm-thick Ag layer was deposited first and 17-nm-thick Al layer - second. The sharp superconducting transition at temperature ~72 mK and <1 mK width between 10% and 90% of the normal resistance was obtained (Fig. 5). The parameter $\alpha \cong 1,200$ was obtained in the cited work and consequently $\tau_{eff}/\tau_{e\rightarrow ph} \cong 1{:}240$ what corresponds to the strong feedback. The *I-V* characteristic and the dependence of dissipated in the absorber-TES power on the bias voltage *V* are shown at Fig. 6. The portion of *I-V* curve with the negative differential resistance and the plateau at the dependence of dissipated power on the bias voltage due to the functioning of the electrothermal feedback correspond to the superconducting transition area.

In the work [20] the estimation of the noise equivalent power of the microbolometer with TES combined with the absorber made on the basis of measurement results at the d.c. is given. The 70×100 $\mu\mathrm{m}^2$ width-to-length and 50 nm-thick Ag/Al bilayer as the absorber-TES having temperature and electrical characteristics close to that shown at Fig. 5 and Fig. 6 was used. Since the replacement of part of d.c. power with the absorbed radiation power takes place in the microbolometer of described type it is easy to derive an expression for the current responsivity: $P_{\mathrm{rad}} = -\Delta I \cdot V$ and the current responsivity $S_{\mathrm{I}} = \Delta I/P_{\mathrm{rad}} = -1/V$ [17]. The beginning of the superconducting transition in the cited work [20] takes place at $V \cong 0.5$ μV and consequently $S_{\mathrm{I}} \cong -2\cdot10^6$ A/W. The measured root-mean-square noise current of the device was $\sqrt{\overline{i_n^2}} \cong 6$ pA$\cdot$Hz$^{-1/2}$ what corresponds approximately to the measurement result obtained in [21] as well. One may obtain the *NEP* of microbolometer from current responsivity and root-mean-square noise current. The result is: $NEP = \sqrt{\overline{i_n^2}}/|S_{\mathrm{I}}| \cong 3\cdot10^{-18}$ W$\cdot$Hz$^{-1/2}$.
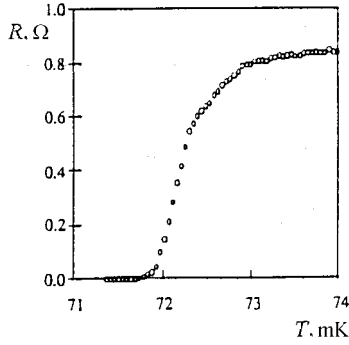
Fig. 5. Characteristic of the superconducting transition of superconductor-normal metal bilayer with proximity effect: 17-nm-thick aluminum layer deposited onto 30-nm-thick silver layer [18].
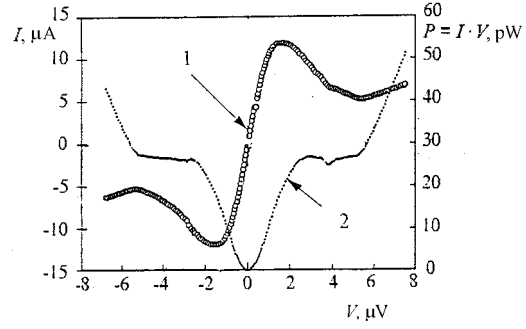
Fig. 6. *I-V* characteristic of the absorber combined with the TES with electrothermal feedback and corresponding dependence of power dissipated in absorber-TES on bias voltage; one may see a plateau at the power of 27 pW on the second dependence: 1 - SQUID current *I*, 2 - power $P = I \cdot V$ [18].

4. Estimation of a maximum possible sensitivity of the microbolometer based on the absorber-TES.

The *NEP* of the radiation detector which utilizes a bulk detection mechanism, for example the heating of electrons or the intrinsic photoeffect (photoconductivity), and has a noise generated in the whole volume of the detector and depending on its resistance, for example the Johnson noise, is proportional to the square root of its volume v [22]:

$$NEP \propto \sqrt{v} \,. \tag{3}$$

The microbolometer under consideration based on the TES combined with absorber utilizes the heating of electrons, i.e. the bulk (volume) effect, and its noise current spectral density is determined by two components [17]:

$$\overline{i_n^2} = \frac{4kT}{R} \cdot \frac{n^2/\alpha^2 + \omega^2 \tau_{eff}^2}{1 + \omega^2 \tau_{eff}^2} + \frac{4kT}{R} \cdot \frac{n/2}{1 + \omega^2 \tau_{eff}^2} \,, \tag{4}$$

where the first component is the Johnson noise and the second one is the phonon noise, i.e. the noise caused by thermal fluctuations during the energy exchange between electrons and phonons. Not going into details we may indicate that both components have similar dependence on the microbolometer resistance *R*. This means that the expression (3) is valid at two said noise components as well. In [10] the same dependence of the *NEP* on v is presented taking into account just the phonon noise what corresponds to the said above.

Using results of measurements of the current sensitivity and the noise current as well as the estimation of the *NEP* of the microbolometer with the TES on the basis of the said

measurements in [20] and expression (3) one may estimate the *NEP* of the microbolometer when its dimensions are decreased. On account of the fixed thickness of the microbolometer ($\cong 50$ nm [20]) which is the thickness sum of both layers of the bilayer determined experimentally under condition of the obtaining the best parameters of the superconducting transition one may modify (3) into

$$NEP \propto \sqrt{l \times w}, \tag{3'}$$

where l is the length and w is the width of the absorber-TES. The results of conversion of the *NEP* of the TES-microbolometer to new dimensions using (3') are given in the Table 1.

The first row of part I (for dimensions $100 \times 70 \, \mu\,\text{m}^2$) is the result of measurements and estimations made in [20]. The second row of part I is the result of the conversion of the *NEP* in accordance with (3') to the dimensions $l \times w \cong 6 \times 0.3 \, \mu\,\text{m}^2$ which has the microbolometer with SIN-junction sensor [8] (see above). We remind that its electrical noise equivalent power is $NEP \cong 3.10^{-18}$ W $\cdot$ Hz$^{-1/2}$ (the same value as in case of the TES-microbolometer with $l \times w = 100 \times 70 \, \mu\,\text{m}^2$!).

Table 1

$l \times w$, $\mu\,\text{m}^2$	NEP, W $\cdot$ Hz$^{-1/2}$
I	
100×70	$\cong 3 \cdot 10^{-18}$ [20]
6×0.3	$\cong 4.8 \cdot 10^{-20}$
0.5×0.2	$\cong 1.4 \cdot 10^{-20}$
II	
1800×900	$\cong 3.3 \cdot 10^{-17}$ [23]
6×0.3	$\cong 3.5 \cdot 10^{-20}$

Result of the conversion of the *NEP* to new dimensions by means of (3') using as a basis the TES-microbolometer described in [23] is given in part II of the Table 1. It has the combined absorber-TES made of tungsten (T$_C$ ~95 mK of W thin film [23]) with $l \times w = 1.8 \times 0.9$ mm^2 and thickness equal to 40 nm connected into the scheme similar to Fig. 3. Its *NEP* is $\cong 3.3 \cdot 10^{-17}$ W $\cdot$ Hz$^{-1/2}$ and the conversion to the dimensions $l \times w = 6 \times 0.3$ $\mu\,\text{m}^2$ gives *NEP* $\cong 3.5 \cdot 10^{-20}$ W $\cdot$ Hz$^{-1/2}$ what is close to the value in the second row of part I.

It is necessary to notice that the noise in [8] was caused not by the microbolometer itself but by the amplifier of the microbolometer output signal and the authors of [8] have estimated that after the reducing the noise of the amplifier by an order the noise will be caused by the intrinsic noise of the SIN-junction sensor what corresponds to an order better (lower) *NEP* $\cong 3 \cdot 10^{-19}$

$W \cdot Hz^{-1/2}$. And even in this case at the same absorber dimensions like in case of the microbolometer with SIN-junction sensor the *NEP* of the microbolometer with absorber-TES will be an order better. This is caused by the fact that whole volume of the absorber-TES is working to generate the output signal of the microbolometer but not just a part of the absorber overlapping with SIN-junction as in case of the microbolometer with SIN-junction sensor. The experimental confirmation of the latter fact is the independence of the output signal of the microbolometer with SIN-junction sensor on the power dissipated in the absorber at two its lengths (Fig. 2): at doubled absorber length l the resistance R is also twice larger and at the same bias current I_b the dissipated power $I_b^2 \cdot R$ in the absorber is also doubled but the microbolometer output signal remains practically unchanged. All said means that the significant portion of hot electrons in the absorber in case of the microbolometer with SIN-junction sensor does not give contribution into the output signal, i.e. the corresponding power is lost (unused) what decreases the effectiveness of this microbolometer in comparison with the microbolometer with TES. It is possible to show this clear with the following judgement. One may assume that instead of one SIN-junction the multiple SIN-junctions are arranged along the whole length of the absorber and all output signal components of the microbolometer are summed by means of a transformer with n primary coils and one secondary coil where n is the amount of SIN-junctions. At 6-μm-long absorber and 0.2-μm-wide SIN-junction (see above) $n \cong 30$. In this case power losses of hot electrons are $\cong$ 29:30 for the single SIN-junction in comparison with thirty SIN-junctions from the viewpoint of the generating of the microbolometer output signal. When the noise of n SIN-junctions is predominating their noise is summed in the transformer as $\sqrt{n \overline{u_{SIN}^2}} = \sqrt{n} \times \sqrt{\overline{u_{SIN}^2}}$, i.e. the noise increases in $\sqrt{n}$ times and the *NEP* becomes better (decreases) proportionally to $\sqrt{n}$: n. When the noise of the amplifier of output signal of the microbolometer is predominating the *NEP* is improved (decreased) proportionally to 1:n. In the case of predominating intrinsic noise of n SIN-sensors with equal noise the *NEP* of SIN-microbolometer with $l \times w = 6 \times 0.3 \, \mu m^2$ will be *NEP* $\cong 3 \cdot 10^{-19} : \sqrt{n}$ $W \cdot Hz^{-1/2} = 3 \cdot 10^{-19} : \sqrt{30}$ $W \cdot Hz^{-1/2} \cong 5.5 \cdot 10^{-20}$ $W \cdot Hz^{-1/2}$ what is close to the *NEP* of the TES-microbolometer with the same absorber dimensions. This means that whole electron temperature increment of SIN-microbolometer absorber is used now for the generating of the output signal. However the creating of a design of the microbolometer with multiple SIN-junctions appears problematic.

The third row in the Table 1 (part I) corresponds to the dimensions $l \times w$ accepted for estimations in the work [10]. In this work the thickness of microbolometer is accepted equal to 10 nm unlike to the case of 50 nm what corresponds to estimation results given in the part I of the Table 1. Besides it was proposed in the cited work to increase an electron energy relaxation time in the absorber-TES up to $\tau_{e \to ph} \sim 10^{-3}$ s due to the significant decreasing of its thickness or/and by the irradiating it with high-energy ions. As the *NEP* depends on the electron energy relaxation time as $(\tau_{e \to ph})^{-1/2}$ [10] it has to be lower in ~70 times in comparison with the value in the third row of the Table 1 on account of said two factors: the decrease of the film thickness in 5 times and the increase of $\tau_{e \to ph}$ approximately from 10^{-6} to 10^{-3} s, i.e. in 10^3 times. This corresponds to *NEP* $\cong 2 \cdot 10^{-22}$ $W \cdot Hz^{-1/2}$ and agrees approximately with estimations in [10]. This impressive value requires a fabrication technology on the height of contemporary technological equipment and moves the Andreev reflection hot-electron microbolometer nearer

to the absolute receiver which *NEP* is determined by the quantum fluctuations of incident radiation [22, 10].

5. The matching of the TES-microbolometer with the incident radiation flow and the output signal read-out channel.

It follows from the analysis made in the previous paragraph that for the achieving the best *NEP* of the Andreev reflection hot-electron microbolometer with the combined absorber-TES one should strive for a minimum possible volume of its working part, i.e. the absorber-TES. It means that dimensions of the absorber-TES have to be chosen much less than the wavelength of the incident radiation. To match so small absorber-TES with the incident radiation flow the optical, to be precise - the quasioptical, focusing of the radiation onto the absorber-TES with said dimensions is impossible because of the radiation diffraction phenomenon on it. By this reason the absorber-TES has to be connected into the center of a planar antenna or into a waveguide. The combination of the quasioptical focusing first, for instance by means of a lens or a horn, and then the matching by means of the planar antenna or the waveguide is possible.

Before a further consideration of the problem of the microbolometer matching with the incident radiation flow and the output signal read-out channel it is necessary to make more detailed estimation of parameters of the microbolometer with the TES as the read-out sensor for instance with dimensions $l \times w = 6 \times 0.3$ μ m^2 using the conversion method already applied above (see Table 1). We accept again the described in paragraph 3 TES-microbolometer with the dimensions $l \times w = 100 \times 70$ μ m^2 as the basis for the conversion. This microbolometer has the d.c. and low frequency resistance $R \cong 0.2$ Ω (approximately like as at Fig. 5). The bilayer is working as a normal metal at frequencies of the incident radiation at $\hbar\omega > \Delta$ where in given case Δ is the energy gap of the superconducting bilayer structure. Besides the absorber-TES thickness is significantly less than skin depth. Owing to these circumstances the bilayer resistance R_ω at the incident radiation frequency ω corresponds to its normal resistance [7], or

$R_\omega = R_n \cong 1 \Omega$. Parameters *V*, $\sqrt{i_n^2}$, S_I and *NEP* of this microbolometer are given above and included into the Table 2 as well, $I = V/R \cong 2.5 \cdot 10^{-6}$ A. We will carry out the conversion of part of these values to the microbolometer with dimensions $l \times w = 6 \times 0.3$ μ m^2 under condition of the constant bilayer thickness as well as the constant current density through it using the following formulas: R and $R_\omega \propto \dfrac{l}{w}$, $I \propto w$, $\sqrt{i_n^2} \propto \sqrt{\dfrac{w}{l}}$ (see (4)). By the way the expression (3') can be derived from these three ones. The rest parameters: *V*, S_I and *NEP* are calculated from first ones. The initial parameters for $l \times w = 100 \times 70 \mu$ m^2 and results of conversion for $l \times w = 6 \times 0.3$ μ m^2 are given in the Table 2. The value of the *NEP* for $l \times w = 6 \times 0.3 \mu$ m^2 coincides with corresponding value in the Table 1 what has to be. The values R, R_ω, V and $\sqrt{i_n^2}$ are primary parameters for the designing of the TES-microbolometer including issues of connection the absorber-TES into the electrical scheme (Fig. 3) and of the matching it with the antenna and the output signal read-out amplifier. The results of the carried out estimation conversion of course have to be approved experimentally.

The experience of the development of submillimeter waveband receivers on the basis of SIS-mixers (see for example [24]) shows that planar antennas are more convenient than waveguides for the purposes of the matching of receiving elements of small dimensions with the incident radiation flow because they may be deposited onto the substrate together with a receiving element, in our case with the microbolometer. Planar antennas can be

Table 2

$l \times w,\ \mu\,\mathrm{m}^2$	100×70	6×0.3
$R,\ \Omega$	0.2	2.8
$R_\omega,\ \Omega$	1.0	14
$I,$ A	$2.5 \cdot 10^{-6}$	$1.1 \cdot 10^{-8}$
$V,$ V	$0,5 \cdot 10^{-6}$	$3 \cdot 10^{-8}$
$\sqrt{\overline{i_n^2}}\ ,\ \mathrm{A} \cdot\ \mathrm{Hz}^{-1/2}$	$6 \cdot 10^{-12}$	$1.6 \cdot 10^{-12}$
$S_I,$ A/W	$-2 \cdot 10^{6}$	$-1/(3 \cdot 10^{-8})$
$NEP,\ \mathrm{W} \cdot \mathrm{Hz}^{-1/2}$	$\cong 3 \cdot 10^{-18}$	$\cong 4.8 \cdot 10^{-20}$

spiral, log-periodic, double-slot [24, 12-14, 25] or of other types. They as it was said are fabricated by microfilm technology methods and the receiving elements are integrated into them. Of course it is necessary to take care of antenna to be made of material with a minimum, better zero, absorption of radiation. It is best of all to fabricate the antenna of a superconductor with the energy gap Δ more than $\hbar\omega$ of the incident radiation so as the antenna material to be superconducting at all incident radiation frequencies. In case when the antenna is made of superconductor its two parts may function as two electrodes as well bringing the bias current into the absorber-TES what will provide the Andreev reflection at the boundaries between the absorber-TES and the antenna. The efficiency of said above antennas is of order of 50% what means that ~50% of the incident radiation flow is absorbed by the matched load in the antenna center [25]. The matching problem of a microbolometer impedance of order of 10-15 Ω or less with the output impedance of the antenna ~120 Ω deposited onto substrate, for instance silicon or quartz, may be solved, for example, by means of the connection between the absorber-TES and the antenna output the microstrip transformer of approximately $\lambda/4$ length, where λ is the wavelength of the incident radiation, fabricated by microfilm technology methods like it was made, for instance, in [24] for the case of SIS-mixer.

The SQUID-picoammeter with the subsequent amplifying stages is the best solution for the measurement of the output signal of the Andreev reflection hot-electron TES-microbolometer because the noise current of the best SQUID-picoammeters is $\sqrt{\overline{i_n^2}} \cong 0.5\ \mathrm{pA} \cdot \mathrm{Hz}^{-1/2}$ [21] what is approximately three times less in comparison with the estimated above intrinsic noise current of the microbolometer at the resistance of units Ohm.

6. Conclusion.

The important results of the first works on investigation of the normal metal hot-electron microbolometer with SIN-junction sensor for the signal read-out are the experimental confirmation of the Andreev reflection of electrons at the boundaries of the normal metal absorber and the superconducting lead electrodes when hot electron energy does not flow out from the absorber to the electrodes as well as the estimation of the noise equivalent power of such microbolometer. As the consequence of review and comparison of research results of different authors on two types of the Andreev reflection hot-electron microbolometer made in the present work the advantage of the superconducting transition-edge sensor (TES) with electrothermal feedback used as the sensor for the read-out the signal of such microbolometer compared with the single SIN-junction sensor for the same purpose is shown. The origin of this advantage is that whole volume of the absorber participates in the generation of the microbolometer output signal in case of the combined absorber-TES when only part of the absorber does this in case of the single SIN-junction sensor. On account of this fact the microbolometer with the TES combined with the absorber has at least one order better (lower) noise equivalent power (*NEP*) in comparison with the microbolometer with the single SIN-junction sensor having the same absorber dimensions. In the same time a design of the microbolometer with multiple SIN-junction sensor looks too complicated and problematic. In the first case the absorber-TES has to be made of a superconductor or as an bilayer of superconductor and normal metal with the proximity effect under condition that its superconducting transition temperature has to be somewhat higher than the microbolometer temperature as well as the bias d.c. current and radiation lead electrodes into the absorber-TES have to be fabricated of a superconductor with the energy gap much higher in comparison with this value of the absorber-TES. The main way to achieve the best *NEP* of said microbolometer is the reducing of absorber-TES dimensions limited by technology possibilities and the application of the planar antennas for the matching of the microbolometer with the incident radiation flow as well as the extralow-noise SQUID-picoammeter with SQUID input coil connected in series with the absorber-TES and fixed bias voltage applied over this series connection for the microbolometer output signal read-out and amplification. The *NEP* of the microbolometer in such version of order of $10^{-20}\,\mathrm{W \cdot Hz^{-1/2}}$ and lower is expected at the existing technological possibilities. At present time experiments for the realization of the proposed solutions are in progress.

References.

1. V.D. Gromov, N.S. Kardashev, V.D. Kurt et al., The Project "Submillimetron", *Scientific Session of the Astro Space Center of the P.N. Lebedev Physics Institute of RAS, Pushchino* (in Russian)*,* (January 1998).
2. L.S. Kuzmin, N.S. Kardashev, V.G. Kurt et al., *Proc. of ESTEC Workshop, Noordwijk,* 127 (November 1998).
3. A.N. Vystavkin, D.V. Chuvaev, T. Claeson et al., *Proc. of 10-th Intern. Symposium on Space Terahertz Technology*, *Charlottesville, USA,* 372 (March 1999).
4. N.D. Whyborn, *Proc. of ESA Symposium devoted to the Far InfraRed and Submillimeter Telescope (FIRST) mission, Grenoble*, *France*, *Institut de Radio Astronomie Millimetrique*, 19 (April 1997).
5. M.J. Griffin, ibid., 31.
6. J.J. Bock, H.G. LeDuc, A.E. Lange, J. Zmuidzinas, ibid., 349.
7. M. Nahum, P.L. Richards, C.A. Mears, *IEEE Trans. Appl. Supercond.* **3**, 2124 (1993).
8. M. Nahum, J.M. Martinis, *Appl. Phys. Lett.* **63**, 3075 (1993).
9. European Space Agency Tender AO3370 "Hot-electron Microbolometer Technology for IR and Sub-mmw Application". Open Date: Oct. 2 (1997).
10. B.S. Karasik, W.R. McGrath, H.G. LeDuc, M.E. Gershenson, *Supercond. Sci. Technol.* **12**, 745 (1999).
11. A.F. Andreev, *Sov. Phys. JETP* **19**, 1228 (1964).
12. A.N. Vystavkin, D.V. Chouvaev, L.S. Kuzmin et al., *Proc. of the 4-th Intern. Conf. on Millimeter and Submillimeter Waves and Applications*, *San Diego*, *USA*, 441 (July 1998).
13. D.V. Chuvaev, L.S. Kuzmin, M.A. Tarasov et al., *Proc. of 9-th Intern. Symposium on Space Terahertz Technology*, *Pasadena*, *USA*, 331 (March 1998).
14. A.N. Vystavkin, D.V. Chouvaev, L.S. Kuzmin et al., *Russian Phys. JETP* **115**, 1085 (1999).
15. M. Nahum, J.M. Martinis, *Appl. Phys. Lett.* **66**, 3203 (1995).
16. J.M. Martinis, *NIM* **A370**, 171 (1996).
17. K.D. Irvin, *Appl. Phys. Lett.* **66**, 1998 **(**1995).
18. K.D. Irwin, G.C. Hilton, J.M. Martinis, B. Cabrera, *NIM* **A370**, 177 (1996).
19. S.W. Nam, B. Cabrera, B. Chugg et al., *NIM* **A370**, 187 (1996).
20. K.D. Irwin, G.C. Hilton, D.A. Wolman, J.M. Martinis, *Appl. Phys. Lett.* **69**, 1945 (1996).
21. A.T. Lee, S.-F. Lee, J.M. Gildemeister, P.L. Richards, *Proc. of 7-th Symp. on Low Temp. Detectors, Munich*, 123 (27 July - 2 August 1997).
22. A.N. Vystavkin, V.V. Migulin, *Radiotekhnika i Elektronika* **12**, 1989 (in Russian) (1967).
23. A.T. Lee, P.L. Richards, S.W. Nam et al. *Appl. Phys. Lett.* **69**, 1801 **(**1996).
24. Yu.V. Belitsky, S.V. Yacobson, L.V. Filippenko at al., *Journal of Communications Technology and Electronics, Russia* **41**, 113 (1996).
25. G.M. Rebeiz, *Proc. of the IEEE* **80**, 1748 (1992).